North Clin Istanb 2023;10(5):636–641
doi: 10.14744/nci.2023.26122

ORIGINAL ARTICLE RADIOLOGY

Differentiating renal cell carcinoma and oncocytoma with volumetric MRI histogram analysis

Ozlem Akinci, Furkan Turkoglu, Mustafa Orhan Nalbant, Ercan Inci

Department of Radiology, Bakirkoy Dr. Sadi Konuk Training and Research Hospital, Istanbul, Turkiye

ABSTRACT

OBJECTIVE: In this study, the utility of histogram parameters derived from diffusion-weighted imaging for differentiate renal cell carcinoma (RCC) from oncocytoma was investigated.

METHODS: This research tracked 126 individuals who were diagnosed with RCC and oncocytoma through histopathological analysis, using magnetic resonance imaging (MRI) assessments from 2015 to 2023. We observed various attributes of these patients, including demographic details, surgical records, pre-surgery MRI results, MRI apparent diffusion coefficient (ADC) histogram analysis, and post-surgery histopathological outcomes. Calculations of ADC measurements such as mean, minimum, and maximum in conjunction with the 5th, 10th, 25th, 50th, 75th, 90th, and 95th quantile points were made. In addition, we also noted the skewness, kurtosis, and variance of these data points.

RESULTS: The focus group for this investigation consisted of 75 male and 51 female patients. Out of these, 82 were diagnosed with RCC and 44 with oncocytoma. All ADC parameters including ADCmin, ADCmedian, ADCmean, and ADCmax, including the 5th, 10th, 25th, 50th, 75th, 90th, and 95th quantile divisions among the oncocytoma cohort were observed to be higher than the corresponding ones in the RCC group. A statistically meaningful difference was discovered between the minimum ADC value along with the 5th ranking of ADC measurements ($p<0.001$), in addition to mean of ADC ($p=0.050$), and the 10th ($p=0.002$) and 25th ($p=0.015$) quantiles of ADC data. When considering the region below the curve (AUC) in ROC analysis, the value of ADCmin was recorded as 0.739, with a sensitivity of 75.0%, and specificity of 68.2%.

CONCLUSION: To distinguish oncocytoma from RCC, it may be useful to conduct a whole-tumor histogram and textural analysis of ADC values.

Keywords: Diffusion-weighted imaging; histogram analysis; magnetic resonance imaging; oncocytoma; renal cell carcinoma.

Cite this article as: *Akinci O, Turkoglu F, Nalbant MO, Inci E. Differentiating renal cell carcinoma and oncocytoma with volumetric MRI histogram analysis. North Clin Istanb 2023;10(5):636–641.*

Before surgery, it is not always possible to distinguish between oncocytoma and renal cell carcinoma (RCC) using diagnostic imaging techniques. While oncocytomas make up 3–7% of solid renal masses, RCC makes up about 80% of all renal tumors among renal masses [1–3]. Oncocytoma imaging findings are usually characterized by homogeneous contrast distribution, a central scar, and washout in the late dynamic venous phases, though these features are not always present [4, 5]. Indeed, oncocytomas and RCC may share some features; for example, in terms of hypovascular appearance, oncocytomas with cystic or hemorrhagic changes may resemble RCC [6].

Diffusion-weighted imaging (DWI) has been newly incorporated into the magnetic resonance imaging (MRI) procedures for the differential diagnosis of renal masses. This addition allows for the non-invasive characterization of tumors [7–9].

Received: July 18, 2023 *Accepted:* September 05, 2023 *Online:* September 27, 2023

Correspondence: Ozlem AKINCI, MD. Bakirkoy Dr. Sadi Konuk Egitim ve Arastirma Hastanesi, Radyoloji Klinig, Istanbul, Turkiye.
Tel: +90 505 628 25 28 e-mail: dr.ozlemgungor@yahoo.com

It is possible to distinguish between kidney lesions (benign and malignant) using DWI's apparent diffusion coefficient (ADC). In the previous studies, ADC values were assessed using manually defined regions of interest (ROIs) on the largest practical section of the tumor, yet it does not accurately reflect the characteristics of diffusion [10, 11].

To evaluate ADC values throughout the lesion without ROI placement, the entire lesion's volumetric ADC histogram is used. Histogram analysis is a statistical tool used to assess the properties of all voxels in a ROI to better estimate the biological characteristics and histological heterogeneity of the tumor [12].

Only a limited number of publications investigated the utility of DWI histogram analysis with respect to the differential diagnosis of oncocytoma and RCC so far. This study aimed to determine whether the ADC histogram and textural analysis can differentiate between oncocytoma and RCC.

Highlight key points

- Diffusion-weighted imaging has recently been shown to be beneficial for the functional assessment of renal malignancies.
- A whole-tumor histogram and textural analysis of ADC values could be useful in distinguishing oncocytoma from RCC.
- It has the potential to increase diagnostic accuracy and contribute to the process of determining an effective treatment approach.

MATERIALS AND METHODS

In this retrospective study, 126 patients who were diagnosed with RCC and oncocytoma following post-operative histopathological examination between January 2015 and December 2023 and who had preoperative MRI images were included in the study. For the study, approval from Bakirkoy Dr. Sadi Konuk Training and Research Hospital Clinical Research Ethics Committee was obtained (approval number: 2023-06-07; approval date: March 20, 2023). The study was conducted in accordance with the Helsinki Declaration.

This study's focus group is composed of 126 patients in total, with 82 of them diagnosed with RCC and the remaining 44 with oncocytoma. The patients who were excluded from this study are those who had no pre-operative MRI, were getting cancer treatment before an MRI examination, had imaging artifacts that make diagnosing lesions more difficult, had an interval between surgery and an MRI examination longer than 1 month, had kid-

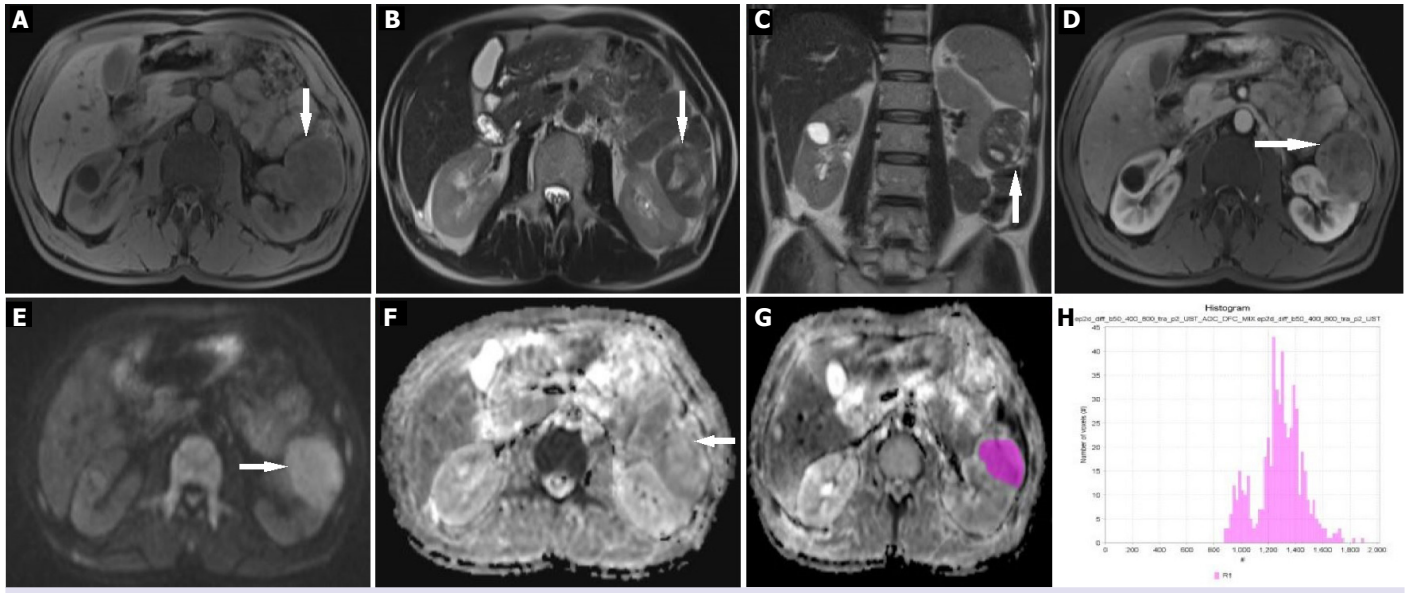

FIGURE 1. A 60-year-old man with clear cell renal cell carcinoma (RCC). **(A)** Low signal intensity on the axial T1-weighted fat suppression image; **(B)** high signal intensity on the axial T2-weighted image; **(C)** high signal intensity on the coronal T2-weighted image; **(D)** high contrast-enhancement on the axial T1-weighted post-contrast fat suppression image; **(E)** concrete restricted diffusion in diffusion-weighted imaging (DWI); **(F)** low ADC on apparent diffusion coefficient (ADC); **(G)** color apparent diffusion coefficient (ADC) map of lesion, the schematic of freehand region of interest (ROI) on diffusion image; and **(H)** corresponding volumetric histogram shows that ADC value was concentrated on the middle of histogram.

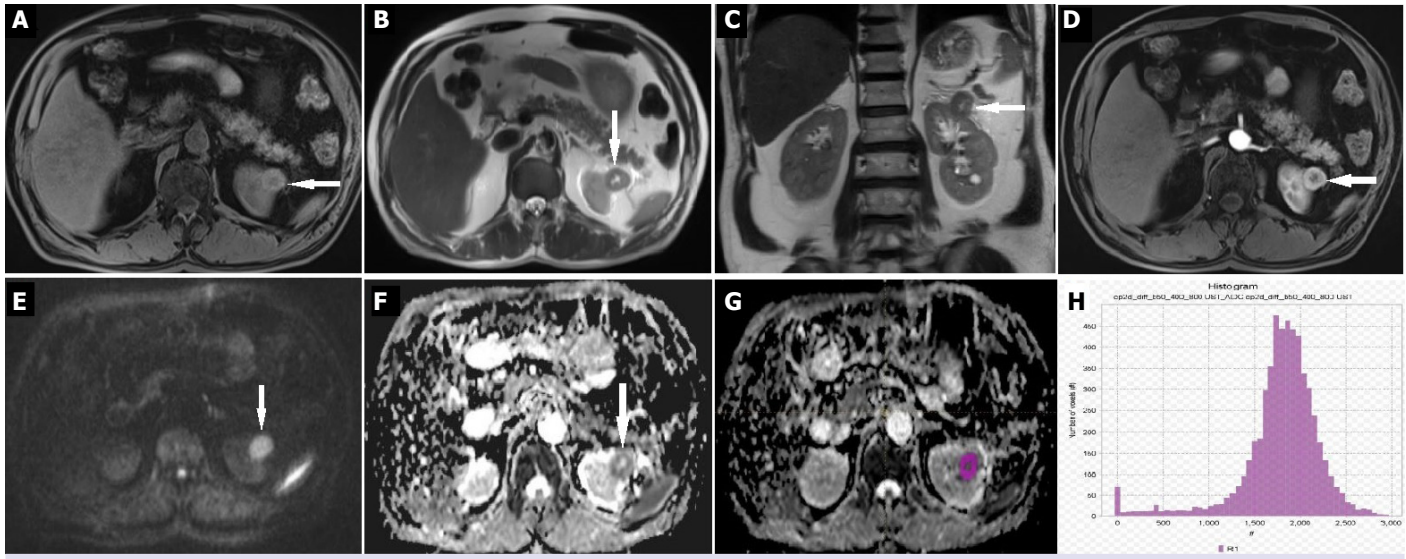

Figure 2. Oncocytoma of the kidney in a 50-year-old man. **(A)** The axial T1-weighted fat suppression image of the lesion exhibits a high signal intensity; **(B)** on the axial T2-weighted image, intermediate signal intensity; **(C)** on the coronal T2-weighted image, intermediate signal intensity; **(D)** on the axial T1-weighted post-contrast fat suppression image, peripheral contrast enhancement, and central necrotic areas; **(E)** diffusion-weighted imaging (DWI) reveals concrete restricted diffusion around the lesion; **(F)** low apparent diffusion coefficient (ADC); **(G)** Lesion color apparent diffusion coefficient (ADC) map, freehand region of interest (ROI) schematic, and diffusion image; and **(H)** ADC value was concentrated on the right of the volumetric histogram, according to the corresponding histogram.

ney surgery in the past for any reason, or had a pathological diagnosis other than RCC or oncocytoma.

Patients' demographic information, MRI results before surgery, MRI ADC histogram analyses, surgical procedures, and post-operative histopathological findings were all documented. Histogram data from MRI ADC scans were compared across study groups.

A 3.0 T magnetic resonance system was employed to capture the signal, employing a 16-channel phased array surface coil from Siemens Medical Solutions, based in Erlagen, Germany. DWI was conducted at b-values of 1000 s/mm². A minimum of 4 h of fasting was required before the MRI. We acquired transverse, sagittal, and coronal thin-section turbo spin-echo T2-weighted (TSE) images (comprising 20 sections, each having a thickness of 3 mm and no intersection gap, with a TR/TE ratio of 5800/100 ms; two signals captured; resolution: 0.8 mm by 0.8 mm). Axial images were captured utilizing breath-induced single instance echo-planar sequences with b-values set at 1000 s/mm² (matrix of 160×192; field of view 0 ranging from 36 to 44 cm; slice thickness of 4 mm; intersection gap of 1 mm; frequency range (kHz/pixel) of 250; capture duration [ms] between 4 and 5; angle of inclination [degrees] of 90; number of excitations of 6).

Table 1. Demographic and radiological data of patients

	RCC n=82 Mean±SD	Oncocytoma n=44 Mean±SD	p
Age	56.22±12.56	59.3±12.1	0.156[a]
Sex (%)			0.124[b]
Male	62.2	54.5	
Female	37.8	45.5	
Tumor diameter (mm)	54.89±32.92	45.63±20.72	0.343[a]

SD: Standard deviation; a: Mann–Whitney U Test; b: Chi-squared test; RCC: Renal cell carcinoma.

Image Analysis

All of the raw data from the DWI was transferred to a personal computer using the picture archiving and communication system. Then, these data were processed by using the free, open-source voxel program LIFEx 7.2.0 (https://lifesoft.org). Two radiologists (each having 8 years of experience in abdominal MRI) reviewed all of the MR scans independently without access to clinical data and histopathologic findings. The radiologists took the

TABLE 2. Comparisons of ADC histogram parameters

ADC (10^{-3} mm^2/s)	RCC	Oncocytoma	Total	p	Significance level
Mean	1.295±0.410	1.451±0.233	1.328±0.383	**0.050**	95%
Standard deviation	0.246±0.133	0.182±0.044	0.233±0.122	**0.024**	95%
Median	1.303±0.427	1.446±0.233	1.334±0.397	0.099	–
Minimum	0.609±0.482	0.962±0.269	0.685±0.467	<**0.0001**	99%
Maximum	1.987±0.618	1.975±0.262	1.984±0.56	0.969	–
Skewness	-0.1±0.6	0.09±0.35	-0.04±0.59	0.242	–
Kurtosis	0.7±1.5	-0.04±0.43	0.52±1.35	**0.019**	95%
5^{th}	0.860±0.407	1.153±0.231	0.923±0.395	<**0.0001**	99%
10^{th}	0.985±0.388	1.221±0.232	1.036±0.373	**0.002**	99%
25^{th}	1.145±0.394	1.325±0.232	1.184±0.372	**0.015**	95%
50^{th}	1.303±0.427	1.446±0.233	1.334±0.397	0.099	–
75^{th}	1.450±0.447	1.577±0.243	1.477±0.414	0.127	–
90^{th}	1.597±0.480	1.690±0.255	1.617±0.442	0.248	–
95^{th}	1.685±0.504	1.758±0.259	1.703±0.465	0.407	–

RCC: Renal cell carcinoma; ADC: Apparent diffusion coefficient.

axial T2-weighted images as a basis to manually draw the ROI covering the lesion in each segment. The data from each ROI were automatically combined into a volumetric ROI which described the entire tumor in voxels (Fig. 1, 2). The following model was then used to create a volumetric ADC map: Diffusion-induced signal attenuation is denoted by S=S0 exp (b ADC). In this formula, S0 represents the signal intensity without diffusion sensitization and b refers to the b value that determines the level of diffusion weighting in the signal. The minimum, maximum, skewness, and variance of ADC values, as well as the 5^{th}, 10^{th}, 25^{th}, 50^{th}, 75^{th}, 90^{th}, and 95^{th} percentiles, were determined. The point on the left showing n% of the voxel values from that histogram is denominated as the nth percentile. Reflecting the deviation of the median from the mean, indicating positive skewness demonstrates indicating a more pronounced or extended right tail of the distribution in comparison to the left tail. The peakiness of the histogram dispense is reflected by kurtosis. High kurtosis distributions are characterized by heavy tails, a sharp peak close to the mean, followed by a rapid decline.

Statistical Analysis

IBM SPSS 23.0 (Chicago, IL, United States) was used for conducting statistical analysis. All patient measurements displayed a distributional variance, as indicated by the histograms. These measurements were utilized to compute mean, minimum, median, maximum, standard deviation, skewness, kurtosis, and percentiles and similar descriptive statistics for each patient group. Moreover, variance in these descriptive statistics was graphically displayed. T-test was applied to independent samples to determine whether these statistical outcomes at the individual level varied between groups. ROC curves were generated based on individual data, and a threshold value was found for the compiled statistical figures. In addition, specificity and sensitivity values were computed for threshold values.

RESULTS

Demographic Data

This study's focus group was composed of 75 males and 51 females (Table 1). Eighty-two of the patients were RCC and 44 were Oncocytoma. There were no statistical differences discovered between the two groups regarding gender and age (p=0.124 and p=0.156, respectively).

Findings Regarding ADC Histogram Parameters

All parameters such as ADCmin, ADCmedian, ADCmean, ADCmax, and the 5^{th}, 10^{th}, 25^{th}, 50^{th}, 75^{th}, 90^{th}, and 95^{th} percentiles for the Oncocytoma group were notably higher than those recorded for the RCC group (Table 2). There was a statistically meaningful difference between ADCmin and the 5^{th} percentile of ADC values

Table 3. ROC results of ADC metrics histogram parameters

Test result variable(s)	AUC	SE[a]	Asymptotic sig.[b]	Asymptotic 95% CI		Cut-off	Sensitivity	Specificity
				Lower bound	Upper bound			
Mean	0.631	0.057	0.050	0.520	0.742	1.486	0.583	0.648
SD	0.651	0.053	0.024	0.245	0.454	0.174	0.583	0.318
Median	0.610	0.056	0.099	0.501	0.719	1.495	0.583	0.670
Minimum	0.739	0.046	<0.0001	0.648	0.830	0.817	0.750	0.682
Maximum	0.497	0.054	0.969	0.392	0.602	1.893	0.667	0.443
Skewness	0.578	0.056	0.242	0.468	0.688	-0.135	0.833	0.466
Kurtosis	0.657	0.053	0.019	0.239	0.446	-0.190	0.708	0.261
5^{th}	0.733	0.049	<0.0001	0.638	0.829	1.028	0.750	0.670
10^{th}	0.704	0.052	0.002	0.602	0.806	1.099	0.708	0.648
25^{th}	0.662	0.056	0.015	0.553	0.771	1.334	0.583	0.670
50^{th}	0.610	0.056	0.099	0.501	0.719	1.495	0.583	0.670
75^{th}	0.602	0.057	0.127	0.490	0.713	1.646	0.542	0.659
90^{th}	0.577	0.057	0.248	0.465	0.690	1.760	0.542	0.614
95^{th}	0.555	0.056	0.407	0.445	0.665	1.861	0.542	0.636

CI: Confidence interval; AUC: Area under the curve; SD: Standard deviation; a: Under the nonparametric assumption; b: Null hypothesis: true area=0.5 The test result variable(s): Kurtosis, p75, p95 has at least one tie between the positive actual state group and the negative actual state group.

($p<0.001$), as well as ADCmean ($p=0.050$), and the 10^{th} ($p=0.002$) and 25^{th} ($p=0.015$) percentiles of ADC values. However, there was no significant statistical difference noted between ADCmedian, ADCmax, and the ADC values from the 50^{th} to 95^{th} percentiles ($p>0.05$).

The RCC group exhibited greater values of variance, skewness, and kurtosis in comparison to the oncocytoma group. There was a statistically significant difference between the variance ($p=0.024$) and kurtosis ($p=0.019$).

Diagnostic Performance

The effectiveness of ADC histogram parameters in diagnosing the oncocytoma group was demonstrated by the ROC curve. The highest area under the curve (AUC) was one of the ADCmin with the value of 0.739. When the cutoff value was set at 0.817×10^{-3} mm²/s, the specificity and sensitivity were 68.2% and 75.0%, respectively. Fifth percentile of the ADC value (AUC=0.733) followed the diagnostic efficacy. Under the threshold of 1.028×10^{-3} mm²/s, the specificity and sensitivity were 67.0% and 75.0%, respectively. With the ADCmean (0.631), 10^{th} (0.704), and 25^{th} (0.662) percentiles of the ADC values, also the AUC was higher. Under the threshold values of 1.486×10^{-3} mm²/s, 1.099×10^{-3} mm²/s, and 1.334×10^{-3} mm²/s, the specificity and sensitivity were 64.8% and 58.3%, 64.8% and 70.8%, and 67.0% and 58.3%, respectively (Table 3).

The AUC demonstrated a higher value when considering the variance (0.651) and kurtosis (0.657). At values below the established thresholds of 0.174×10^{-3} mm²/s and -0.190, the specificity and sensitivity were determined to be 31.8% and 58.3% and 26.1% and 70.8%, respectively (Table 3).

DISCUSSION

At present, a notable proportion of non-malignant renal masses is detected incidentally during histopathological evaluations of individuals who have had resection procedures, ranging from 10% to 30 [13].

A meta-analysis by Tordjman et al. [12] found that compared to ADC of the entire lesion, ADC of renal tumors that exclude necrotic and cystic regions was more accurate at differentiating between RCC and other renal lesions.

In our study, the oncocytoma group's ADCmin, ADCmedian, ADCmean, ADCmax, 5^{th}, 10^{th}, 25^{th}, 50^{th}, 75^{th}, 90^{th}, and 95^{th} percentiles were all higher than those of the RCC group. This finding is consistent with

the relevant literature, as also previous publications on this topic came up with similar results [14–16].

The asymmetry of the histogram is referred to as the skewness [17]. Based on ADC maps, Kierans et al. [18] discovered that the skewness of ccRCC was significantly greater in high-stage tumors than in low-stage tumors, suggesting that ADC texture analysis to be conducted on ccRCC can be used as a noninvasive method to detect high-stage tumors accurately on preoperative imaging.

In this study, the RCC group exhibited greater values of variance, skewness, and kurtosis in comparison to the oncocytoma group. There was a statistically significant difference between the variance (p=0.024) and kurtosis (p=0.019). It showed that the majority of RCC ADC values were clustered to the left of the histogram in the low ADC values region, whereas the majority of oncocytoma ADC values were clustered to the right of the histogram in the high ADC values area. One can avoid from unnecessary surgical approaches to diagnose renal masses completely if high-DWI techniques such as high-ultra-high-b-value DW images and diffusion tensor imaging could be improved and advanced [19].

Our research included a number of limitations and strengths. First, a limited number of people participated in the research. Second, because this was a retrospective study, there were naturally occurring biases in the selection of patients. Our use of whole-tumor ROI, which boasts superior reproducibility compared to single-slice ROI, was one of the key factors that contributed to the success of our research.

Conclusion

The present study showed that textural analysis of ADC values and a whole-tumor histogram could be useful in distinguishing oncocytoma from RCC. It has the potential to increase diagnostic accuracy and contribute to the process of determining an effective treatment approach.

Ethics Committee Approval: The Bakirkoy Dr. Sadi Konuk Training and Research Hospital Clinical Research Ethics Committee granted approval for this study (date: 20.03.2023, number: 2023-06-07).

Conflict of Interest: No conflict of interest was declared by the authors.

Financial Disclosure: The authors declared that this study has received no financial support.

Authorship Contributions: Concept – OA, MON; Design – OA; Supervision – EI; Materials – FT, MON; Data collection and/or processing – FT, MON; Analysis and/or interpretation – OA, EI; Literature review – OA, FT; Writing – OA; Critical review – EI.

REFERENCES

1. Mytsyk Y, Dutka I, Borys Y, Komnatska I, Shatynska-Mytsyk I, Farooqi AA, et al. Renal cell carcinoma: applicability of the apparent coefficient of the diffusion-weighted estimated by MRI for improving their differential diagnosis, histologic subtyping, and differentiation grade. Int Urol Nephrol 2017;49:215–24. [CrossRef]
2. Yu X, Lin M, Ouyang H, Zhou C, Zhang H. Application of ADC measurement in characterization of renal cell carcinomas with different pathological types and grades by 3.0 T diffusion-weighted MRI Eur J Radiol 2012;81:3061–6. [CrossRef]
3. Lassel E, Rao R, Schwenke C, Schoenberg S, Michaely H. Diffusion-weighted imaging of focal renal lesions: a meta-analysis. Eur Radiol 2014;24:241–9.
4. Gakis G, Kramer U, Schilling D, Kruck S, Stenzl A, Schlemmer HP. Small renal oncocytomas: differentiation with multiphase CT. Eur J Radiol 2011;80:274–8. [CrossRef]
5. Cornelis F, Lasserre AS, Tourdias T, Deminiere C, Ferriere JM, Bras YL, et al. Combined late gadolinium-enhanced and double echo chemical-shift MRI help to differentiate renal oncocytomas with high central T2 signal intensity from renal cell carcinomas. Am J Roentgenol 2013;200:830–8. [CrossRef]
6. Zhang J, Lefkowitz RA, Ishill NM, Wang L, Moskowitz CS, Russo P, et al. Solid renal cortical tumors: differentiation with CT. Radiology 200;244:494–504. [CrossRef]
7. Chen LS, Zhu ZQ, Wang ZT, Li J, Liang LF, Jin JY, et al. Chemical shift magnetic resonance imaging for distinguishing minimal-fat renal angiomyolipoma from renal cell carcinoma: a meta-analysis. Eur Radiol 2018;28:1854–61.
8. Just N. Improving tumour heterogeneity MRI assessment with histograms. Br J Cancer 2014;111:2205–13. [CrossRef]
9. Li XL, Shi LX, Du QC, Wang W, Shao LW, Wang YW. Magnetic resonance imaging features of minimal-fat angiomyolipoma and causes of preoperative misdiagnosis. World J Clin Cases 2020;8:2502–9. [CrossRef]
10. Chen CL, Tang SH, Wu ST, Meng E, Tsao CW, Sun GH, et al. Calcified, minimally fat-contained angiomyolipoma clinically indistinguishable from a renal cell carcinoma. BMC Nephrol 2013;14:160. [CrossRef]
11. Hindman N, Ngo L, Genega EM, Melamed J, Wei J, Braza JM, et al. Angiomyolipoma with minimal fat: can it be differentiated from clear cell renal cell carcinoma by using standard MR techniques. Radiology 2012;265:468–77.
12. Tordjman M, Mali R, Madelin G, Prabhu V, Kang SK. Diagnostic test accuracy of ADC values for identification of clear cell renal cell carcinoma: systematic review and meta-analysis. Eur Radiol 2020;30:4023–38. [CrossRef]
13. Lane BR, Babineau DC, Poggio ED, Weight CJ, Larson BT, Gill IS, et al. Factors predicting renal functional outcome after partial nephrectomy. J Urol 2008;180:2363–8. [CrossRef]
14. Anna K, Paschall S, Mirmomen M, Pourmorteza A, Gautam R, Sahai A, et al. Differentiating papillary type I RCC from clear cell RCC and oncocytoma: application of whole lesion volumetric ADC measurement. Abdom Radiol 2018;43:2424–30. [CrossRef]
15. Taouli B, Thakur RK, Mannelli L, Babb JS, Kim S, Hecht EM, et al. Renal lesions: characterization with diffusion-weighted imaging versus contrast-enhanced MR imaging. Radiology 2009;251:398–407. [CrossRef]
16. Wang H, Cheng L, Zhang X, Wang D, Guo A, Gao Y, et al. Renal cell carcinoma: diffusion-weighted MR imaging for subtype differentiation at 3.0 T. Radiology 2010;257:135–43. [CrossRef]
17. Zhang Y, Chen J, Liu S, Shi H, Gun W, Ji C, et al. Assessment of histological differentiation in gastric cancers using whole-volume histogram analysis of apparent diffusion coefficient maps. J Magn Reson Imaging 2017;45:440–9.
18. Kierans AS, Rusinek H, Lee A, Shaikh MB, Triolo M, Huang WC, et al. Textural differences in apparent diffusion coefficient between low-and high-stage clear cell renal cell carcinoma. AJR Am J Roentgenol 2014;203:6376–44. [CrossRef]
19. Shafiee MJ, Haider AS, Wong A, Lui D, Cameron A, Modhafar A, et al. Apparent ultra-high b-value diffusion-weighted image reconstruction via hidden conditional random fields. IEEE Trans Med Imaging 2015;34:1111–24.